Extrinsic Precursor-Assisted Synthesis of 1,5-Hexadiene on Cu(100)

H. Celio, K. C. Scheer, and J. M. White*

Contribution from the Center for Materials Chemistry, Department of Chemistry and Biochemistry, University of Texas at Austin, Austin, Texas 78712-1167

Received March 31, 2000

Abstract: The reaction between allyl bromide and previously chemisorbed η^3-allyl to form 1,5-hexadiene on Cu(100) at cryogenic temperatures has been examined using reflection absorption infrared spectroscopy and temperature-programmed desorption. Above 110 K, the 1,5-hexadiene formation rate decreases with increasing temperature and is controlled by the residence time of dosed allyl bromide, whereas below 100 K, the rate increases with temperature and is controlled by the reaction of weakly adsorbed allyl bromide with chemisorbed η^3-allyl. Above 110 K, a precursor state model is used to interpret the data. The activation energy difference, $E_d - E_r$, between desorption and reaction of allyl bromide with η^3-allyl is 12 kJ mol^{-1}.

I. Introduction

The study of transition metal-catalyzed carbon−carbon bond-forming reactions constitutes a major area of fundamental research and technological significance, e.g., Fischer−Tropsch synthesis[1] and oxidative coupling of methane.[2] For these and other catalyzed coupling processes, overall reaction paths have been proposed, but mechanistic details are sparse.[1,2] Typically, Langmuir−Hinshelwood, Rideal−Eley, and precursor mechanisms have used to describe adsorption and reaction of hydrocarbons on clean transition metal and nonmetallic surfaces.[3]

While the concept of transient precursor states, proposed four decades ago by Kisliuk,[4] is often used to describe impinging reactants, characterizing the reaction kinetics of extrinsic precursors remains challenging.[3] Two types of precursors, intrinsic and extrinsic, are distinguished on the basis of whether the weakly adsorbed precursor molecule, trapped (physisorbed) by dispersion forces, is located over an empty substrate site (intrinsic) or over an adsorbate layer site (extrinsic). Kisliuk originally proposed an intrinsic precursor state to explain the dissociative adsorption kinetics of nitrogen over tungsten.[4] More recently, intrinsic precursor states have been identified in the process of forming chemisorbed benzene on Si(111)−7 × 7[5] and in the kinetics of ethane dissociation on Si(100)−(2 × 1) and Ir(110)−(1 × 2).[6,7] Theoretical studies of both extrinsic and intrinsic precursor states are also available.[8]

In a recent Communication,[9] we reported the facile formation of 1,5-hexadiene, C_6H_{10}, at cryogenic temperatures (110 K) while dosing allyl bromide, C_3H_5Br, on Cu(100) covered with η^3-allyl species and atomic bromine. This cryogenic coupling reaction contrasts with typical carbon−carbon coupling reactions of adsorbed alkyl and vinyl groups on Cu and other transition metals under ultrahigh-vacuum (UHV) conditions.[10,11] The Communication also included the first high-resolution reflection absorption infrared spectrum (RAIRS) of chemisorbed η^3-allyl, an important C_3 species.[12,13]

Other substrates, e.g., Pt(111),[15,24] Al(100),[16] Ag(111),[17] Ag(110),[18] and Ni(100),[19] have been used in surface science investigations of allyl groups formed from allyl halides. For example, in a recent study of C_3H_5Br and C_3H_5I on Pt(111),[24] RAIRS and TPD indicated the formation of η^1- and η^3-C_3H_5 following cleavage of the carbon−halogen bond. The products formed in TPD depended on coverage; at low coverages, no C-containing species desorbed, but at high coverages some propene desorbed. The latter occurred in two TPD peaks. The lower (185 K) was attributed to prompt desorption upon H addition to η^1-C_3H_5 and the higher (250 K) to the hydrogenation of η^3-C_3H_5 to a di-σ form of propene that undergoes significant D-for-H exchange prior to desorbing as propene. There was no evidence in this study for C−C bond formation.

Here, we report further on the coupling reaction that forms 1,5-hexadiene, focusing on the mechanism and temperature dependence of its kinetics. Dissociative adsorption of allyl chloride, C_3H_5Cl, was used to prepare a saturated and well-

* Corresponding author. Tel.: 512-471-3704. Fax: 512-471-9495. E-mail: jmwhite@mail.utexas.edu.

(1) Anderson, R. B. *The Fischer−Tropsch Synthesis*; Academic Press: London, U.K., 1984.
(2) Somorjai, G. A. *An Introduction to Surface Chemistry and Catalysis*; Wiley-Interscience: New York, 1994; Chapter 7.
(3) Masel, R. I. *Principles of Adsorption and Reaction on Solid Surfaces*; Wiley: New York, 1996; Chapter 10.
(4) Kisliuk, P. *J. Phys. Chem. Solids* **1957**, *3*, 95−101.
(5) Brown, D. E.; Moffatt, D. J.; Wolkow, R. A. *Science* **1998**, *279*, 542−544.
(6) Reeves, C. T.; Ferguson, B. A.; Mullins, C. B.; Sitz, G. O.; Helmer, B. A.; Graves, D. B. *J. Chem. Phys.* **1999**, *111*, 7567−7575.
(7) (a) Kang, H. C.; Mullins, C. B.; Weinberg, W. H. *J. Chem. Phys.* **1990**, *92*, 1397−1406. (b) Soulen, S. A.; Madix, R. J. *Surf. Sci.* **1995**, *323*, 1−5.
(8) (a) Doren, D. J.; Tully, J. C. *Langmuir* **1988**, *4*, 256−268. (b) Doren, D. J.; Tulley, J. C. *J. Chem. Phys.* **1991**, *94*, 8428−8440.
(9) Celio, H.; Smith, K. C.; White, J. M. *J. Am. Chem. Soc.* **1999**, *121*, 10422−10423.
(10) Bent, B. E. *Chem. Rev.* **1996**, *96*, 1361−1390.
(11) Zaera, F. *Chem. Rev.* **1995**, *95*, 2651−2693.
(12) (a) Biloen, P.; Helle, N. J.; Sachtler, W. M. H. *J. Catal.* **1979**, *58*, 95−107. (b) Brady, R. C., III; Pettit, R. *J. Am. Chem. Soc.* **1981**, *103*, 1287−1289.
(13) Maitlis, P. M.; Long, H. C.; Quyoum, R.; Turner, M. L.; Wang, Z. Q. *Chem. Commun.* **1996**, 1−8.
(14) Collman, J. P.; Hegedus, L. S.; Norton, J. R.; Finke, R. G. *Principles and Applications of Organotransition Metal Chemistry*; University Science Books: Mill Valley, CA, 1987; Chapter 19.
(15) Scoggins, T. B.; White, J. M. *J. Phys. Chem.* **1997**, *101*, 7958−7967.
(16) Bent, B. E.; Nuzzo, R. G.; Zegarski, B. R.; Dubois, L. H. *J. Am. Chem. Soc.* **1991**, *113*, 1143.
(17) Kershen, K.; Celio, H.; Lee, I.; White, J. M. *Langmuir* **2001**, *17*, 323−328.
(18) Dvorak, J.; Dai, H. L. *J. Chem. Phys.* **2000**, *112*, 923−934.
(19) Tjandra, S.; Zaera F. *J. Phys. Chem. B* **1997**, *101*, 1006.

10.1021/ja0011414 CCC: $20.00
Published on Web 03/09/2001

characterized 1:1 layer of chemisorbed η^3-C_3H_5 and Cl with which impinging C_3H_5Br forms a precursor state and reacts to form physisorbed C_6H_{10} as follows:

$$C_3H_5Br_{(p)} + \eta^3\text{-}C_3H_{5(c)} + Cl_{(c)} \rightarrow C_6H_{10(p)} + Br_{(c)} + Cl_{(c)} \quad (1)$$

The subscripts (p) and (c) denote physisorbed and chemisorbed states, respectively. The reactive sticking probabilities of incident C_3H_5Br were extracted using an analogue of the King and Wells method[20−22] based on reflection absorption infrared spectroscopy (RAIRS). In a related work to be published elsewhere,[23] we show that for a surface saturated with $C_3H_{5(c)}$ and the accompanying halogen as in (1), C_3H_5 takes the *exo*-η^3- form between 77 and 300 K, i.e., all three carbons bound to Cu (η^3) and oriented so the C−C−C angle is pointed away from the accompanying halogen (*exo*). Further, temperature-programmed desorption (TPD) is dominated by C_3H_5 radical desorption at ∼450 K.

Using RAIRS data, complemented by TPD data, and the rich literature that describes organometallic reaction chemistry of allyl groups (e.g., coupling reactions between η^3-C_3H_5 groups),[14] we answer two fundamental questions. First, how does C_3H_5Br adsorb on a 1:1 layer of η^3-$C_3H_{5(c)}$ and $Cl_{(c)}$? Second, what kinetics and mechanism describe the reaction between C_3H_5Br and η^3-$C_3H_{5(c)}$ to form physisorbed 1,5-hexadiene, C_6H_{10}?

II. Experimental Section

The experiments were performed in a two-level ultrahigh-vacuum (UHV) chamber with a base pressure of 4×10^{-10} Torr. The lower chamber is equipped with standard surface analysis tools, including a single-pass cylindrical mirror analyzer for Auger electron spectroscopy (AES) and a differentially pumped quadrupole mass spectrometer for TPD. The upper chamber houses a residual gas analyzer (RGA) and is coupled to a commercial Fourier transform infrared spectrometer for RAIRS. Infrared spectra (peak-to-peak noise ∼0.004% $\Delta R/R$ units) were recorded by co-adding 1500 scans at 4 cm^{-1} resolution. All spectra are reported with respect to an appropriate reference that accounts for differing reflectivities (e.g., electronic absorption). The reference was either clean Cu(100) or halogen-covered Cu(100). The Cu(100) temperature was varied between 77 and 1000 K using a power supply controlled by feedback from a type K thermocouple inserted into the edge of the crystal.

The surface was cleaned by cycles of Ar^+ ion grazing-incidence sputtering at 750 K (1.5 kV, 8 μA, 15 min) and annealing (975 K for 15 min). Cycles continued until impurity (C, O, Si, and S) concentrations were below AES detection limits. A more stringent quality test, RAIRS of adsorbed CO,[25] confirmed both cleanliness and surface ordering with minimal defects.

The adsorbates, allyl bromide (3-bromopropene, C_3H_5Br, Aldrich 98+%; stabilized with propylene oxide), allyl chloride (3-chloropropene, C_3H_5Cl, Aldrich 99+%; stabilized with propylene oxide), and 1,5-hexadiene (Aldrich 99+%), were each purified by several freeze−pump−thaw cycles prior to each experiment. Reproducible dosing, through a cylindrical tube (3 mm i.d., 60 mm in length) that terminated 3 cm in front of the Cu(100) surface, was achieved using an altered version of the common procedure. Rather than opening and closing the variable leak valve, we preset it and left it open at all times. With the sample holder and substrate at 300 K, the leak valve was set so that the pressure inside the chamber rose to 4×10^{-9} Torr when 100 mTorr of Ar was applied to it. This pressure was used to calculate doses in Langmuir (1 L = 1×10^{-6} Torr·s), e.g., a 0.6 L dose of C_3H_5Br requires a 150 s exposure. To dose, 100 mTorr of gas was first placed in a vessel behind a butterfly valve (closed) that was connected by an evacuated tube to the preset leak valve. The butterfly valve was then opened. The dose terminated by evacuating the gas behind the leak with the butterfly valve open. This procedure improved the reproducibility of the coverages compared to the typical procedure of opening and closing the leak valve. It is noteworthy that, with the sample holder and substrate at cryogenic temperatures and the same doser settings, the pressure rose to no more than 6×10^{-10} Torr when dosing the allyl-containing molecules.

To prepare the $C_3H_{5(c)}$ and $Cl_{(c)}$ layer, 1.0 L of C_3H_5Cl was dosed on clean Cu(100) at 110 K, annealed to 200 K to desorb excess C_3H_5Cl, and cooled to the temperature of interest. This procedure yielded highly reproducible infrared spectra of $C_3H_{5(c)}$ and $Cl_{(c)}$ that were saturated with respect to further dissociation of dosed C_3H_5Cl.

Cl-covered Cu(100) without $C_3H_{5(c)}$ was prepared by dosing C_3H_5Cl at 110 K and annealing to 550 K to desorb C_3H_5. After three dose/anneal cycles, the Cl/Cu AES ratio saturates, and there is no RAIRS evidence for dissociation upon dosing and annealing more C_3H_5Cl. To prepare bromine-covered Cu(100), the same procedure was followed using C_3H_5Br. The extremely weak bromine Auger signal (LMM transition at 1393 eV) precludes a direct assessment of the number of cycles required to reach saturation.

As noted in the Introduction, we used a method related to that frequently used in molecular beam scattering to extract precursor reaction kinetics.[22] Using RAIRS, we monitored the intensity of $C_3H_{5(c)}$ for active and inactive surfaces and used the ratio to compute the reaction probability (S_r). S_r is analogous to the sticking probability (S), typically measured with mass spectrometry. However, unlike mass spectrometry, which monitors desorbed species, RAIRS monitors surface species. The details of this procedure will be described below in the context of the RAIRS data.

III. Results

Multilayer C_3H_5Cl dosed at 110 K, annealed to 200 K, and recooled to 110 K leaves a surface covered with equal and saturated concentrations of $C_3H_{5(c)}$ and $Cl_{(c)}$ but no C_3H_5Cl.[30] The RAIRS, Figure 1A, comprises a strong band at 886 cm^{-1} assigned to η^3-$allyl_{(c)}$,[9] and two peaks at 2089 and 2114 cm^{-1}. The latter are inverted, indicating their presence in the reference spectrum, and are assigned to CO adsorbed on step edges.[25] This CO accumulates primarily during the collection of the background RAIRS at 110 K, 65 degrees below the desorption temperature of CO.[25]

Spectrum B, which uses the same reference as spectrum A, was taken after dosing 2.0 L of CO on the saturated 1:1 η^3-$C_3H_{5(c)}$ and $Cl_{(c)}$ overlayer. Differences between A and B are negligible, indicating strong inhibition of CO adsorption. Even after a 10 L CO dose, there is no RAIRS change (not shown). For spectrum C, system B was annealed to 550 K in a vacuum, recooled to 110 K, and dosed with 2.0 L of CO. As expected, there is no η^3-$allyl_{(c)}$ signal. There is, however, an intense, narrow band (full width at half-maximum (fwhm) = 7.5 cm^{-1}) at 2091 cm^{-1} assigned to CO by comparing it with the spectrum of CO-saturated ($\theta_{CO} = 0.57$) Cu(100).[25] The integrated CO intensity, $I_{(CO)} \cong \int(\Delta R/R)\, d\nu$, is 0.20 ± 0.01 cm^{-1} compared to 0.30 ± 0.01 cm^{-1} for saturation CO on clean Cu (not shown). In the Discussion section, we estimate the coverage of the 1:1 η^3-$allyl_{(c)}$ and $Cl_{(c)}$ overlayer using the CO intensities from these experiments.

Figure 2 shows RAIRS, each from a separate experiment, of a saturation 1:1 η^3-$allyl_{(c)}$ and $Cl_{(c)}$ prepared as described above—

(20) King, D. A.; Wells, M. G. *Surf. Sci.* **1972**, *29*, 454−482.
(21) (a) King, D. A. In *Critical Reviews in Solid State and Materials Sciences*; Schuele, D. E., Hoffman, R. W., Eds.; CRC Press: Boca Raton, FL, 1978; pp 167−208. (b) Arumainayagam, C. R.; Madix, R. J. In *Molecular Beam Studies of Gas-Phase Collision Dynamics*; Davidson, S. G., Ed.; Progress in Surface Science 38; Pergamon: New York, 1991; pp 1−102.
(22) Cassuto, A.; King, D. A. *Surf. Sci.* **1981**, *102*, 388−404.
(23) Celio, H.; White, J. M. *J. Phys. Chem.*, in press.
(24) Chrysostomou, D.; Zaera, F. *J. Phys. Chem.* **2001**, *105*, 1003−1011.
(25) (a) Uvdal, P.; Karlsson, P.-A.; Nyberg, C.; Andersson, A.; Richardson, N. V. *Surf. Sci.* **1988**, *202*, 167−182. (b) Hollins, P. *Surf. Sci. Rep.* **1992**, *16*, 51−94.

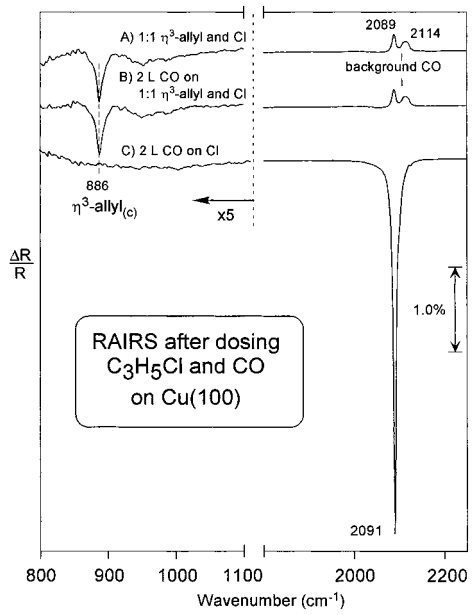

Figure 1. RAIRS 1:1 mixture of η^3-allyl$_{(c)}$ and Cl$_{(c)}$ (A), followed by dosing 2.0 L CO (B) and 2 L CO on Cl-covered Cu(100) after desorption of η^3-allyl$_{(c)}$ groups (C). The inverted peaks in spectra A and B near the 2100 cm^{-1} region are due to background CO adsorption on clean Cu(100). All spectra were taken at 110 K, and the ordinate in the region between 800 and 1100 cm^{-1} was multiplied by 5.

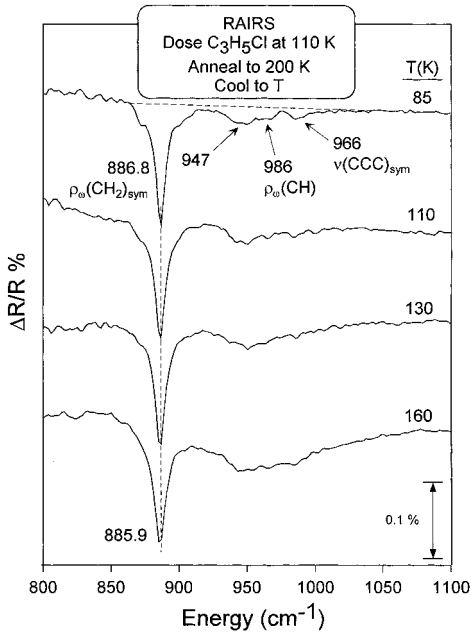

Figure 2. Reflection absorption infrared spectra (RAIRS) of a saturation 1:1 mixture of η^3-C$_3$H$_{5(c)}$ and Cl$_{(c)}$ on Cu(100) at temperatures between 85 and 160 K. The adsorbate layer was prepared by dosing 1.0 L C$_3$H$_5$Cl at 110 K, annealing at 200 K to desorb undissociated C$_3$H$_5$Cl, and cooling to the indicated temperatures. Spectra were acquired by adding 1500 scans at 4.0 cm^{-1} resolution.

dose at 110 K, anneal to 200 K, and cool to indicated *T* for RAIRS. While taken at 10 K intervals, only four spectra are shown. The bands of the 85 K spectrum in Figure 2 support a previously proposed,[9] single-isomer, homogeneously bound η^3-C$_3$H$_{5(c)}$ structure consistent with that found for metal complexes. The same bands appear upon dissociating allyl bromide on Cu(100).[9] There is little temperature dependence, from which we conclude that a 200 K anneal followed by cooling to temperatures between 85 and 160 K leads to the same η^3-C$_3$H$_{5(c)}$ + Cl$_{(c)}$ structure. The relatively narrow 886 cm^{-1} band is characteristic of a homogeneous environment and suggests an intimately mixed and ordered overlayer of η^3-C$_3$H$_{5(c)}$ + Cl$_{(c)}$. In particular, between 85 and 160 K, this band red-shifts by no more than 1 cm^{-1}, the fwhm increases slowly from 7.8 to 11.8 cm^{-1}, and there is no detectable line shape change. The integrated intensity, $(9.5 \pm 0.3) \times 10^{-3}$ cm^{-1}, also shows little variation. The other bands are too weak for us to assess the effect of substrate temperature, but there is no evidence for significant changes. Discussion of the weak band at ~947 cm^{-1} is postponed to the Discussion section.

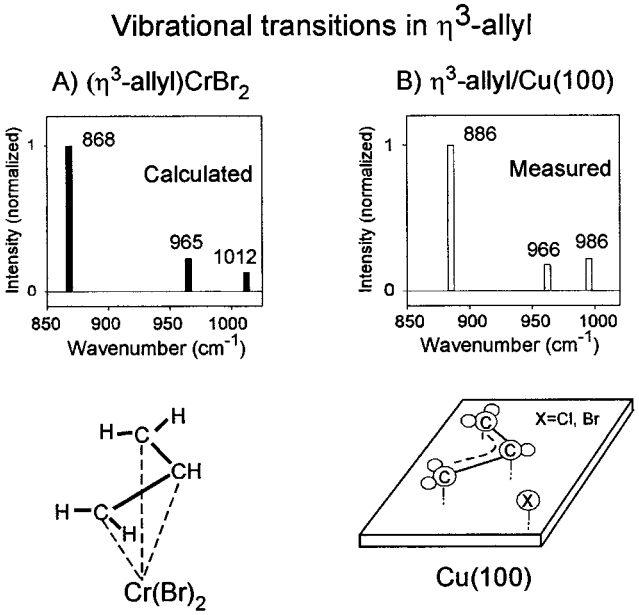

Figure 3. Bar graphs comparing vibrational bands calculated for a Cr metal complex (A) and observed for η^3-allyl on Cu(100) (B). The proposed bonding structures for each case are also displayed.

The band assignments in Figure 2 are based on a density functional theory study of an (η^3-allyl)CrBr$_2$ complex[41] that assigns the 887, 966, and 986 cm^{-1} transitions to ρ_ω(CH$_2$)$_{sym}$, ρ_ω(CH), and ν(CCC)$_{sym}$ modes with A' symmetry (C_s local symmetry[27]). Figure 3 compares the positions and integrated intensities of the two cases (normalized to the strong band between 868 and 886 cm^{-1}). The Cu(100) data were fit using Lorentzian (886 cm^{-1} peak) and Gaussian (966 and 986 cm^{-1} peaks) functions.[28] Agreement is excellent, lending support to the η^3-allyl structural assignment on Cu(100).

The (η^3-allyl)Cr(Br)$_2$ complex (geometry indicated in Figure 3A) contains a delocalized C−C−C framework (C−C−C bond angle is 122° and C−C bond lengths are ~1.4 Å) π-bonded (dashed lines) to the Cr center.[41] The plane of the allyl moiety is canted at an angle of 5−10° with respect to the coordination polyhedron around the Cr atom. This calculated structure and bonding configuration is in excellent agreement with well-established π-bonded allyl complexes, e.g., bis(η^3-allyl) nickel.[42] The orientation of the η^3-allyl on Cu(100) comes from a near-edge X-ray absorption fine structure (NEXAFS) measurement that places the C−C−C plane nearly parallel to the metal

(26) Sheppard, N.; De La Cruz, C. *Adv. Catal.* **1996**, *41*, 1−122.

(27) In C_s symmetry, the 18 vibrational modes of an allyl group are distributed as 10A′ and 8A″, where A′ represents the totally symmetric modes and A″ represents the non-totally symmetric modes. Based on the surface selection rule, all of the A′ modes are infrared active and the A″ modes are infrared inactive.

(28) The peaks were fit with a commercial software package: *Peak Fit*; Jandel: Chicago, IL, 1991.

(29) Durig, J. R.; Jalilian, M. R. *J. Phys. Chem.* **1980**, *84*, 3543−3547.

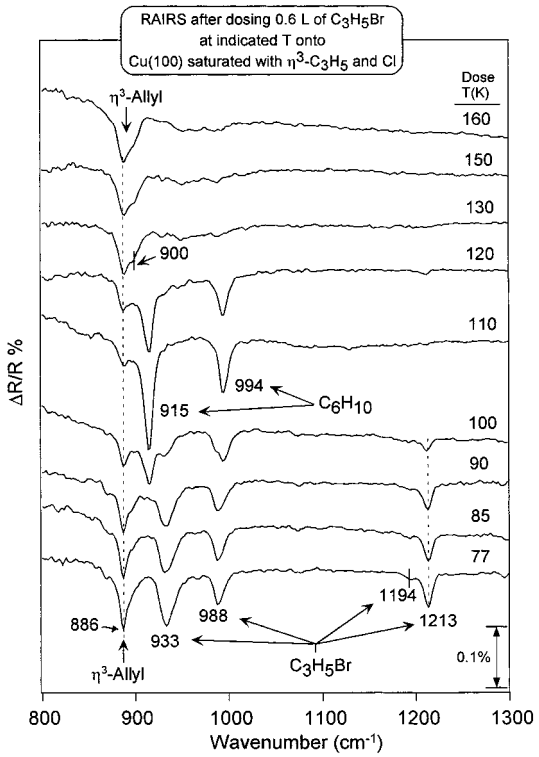

Figure 4. RAIR spectra of allyl bromide (0.6 L) dosed at different temperatures on Cu(100) saturated with a 1:1 mixture of η^3-$C_3H_{5(c)}$ and $Cl_{(c)}$. Reaction of $C_3H_5Br_{(p)}$ and η^3 -C_3H_5 produces 1,5-hexadiene, $C_4H_{10(p)}$. Bands assigned to various species are marked.

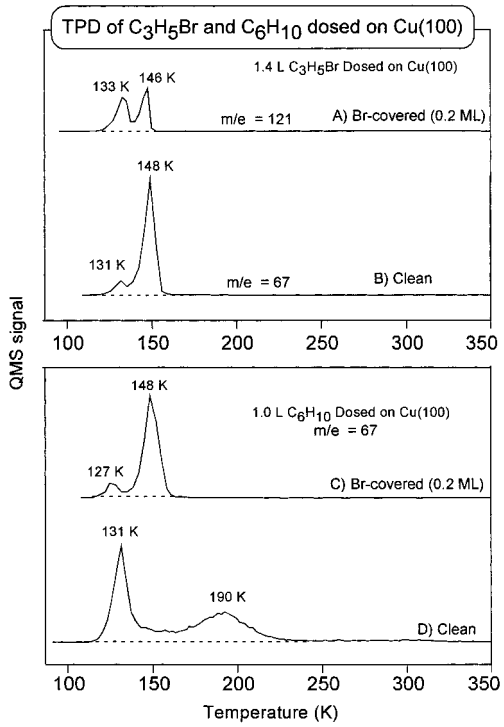

Figure 5. (Top) TPD spectra of a 1.4 L dose of C_3H_5Br on (A) ~0.2 ML Br-covered and (B) clean Cu(100). (Bottom) (C) 1.0 L 1,5-hexadiene dosed on Br-covered Cu(100) and (D) 2.0 L 1,5-hexadiene dosed on clean Cu(100). The adsorption temperature for each spectrum was 110 K, and the heating rate was 2.5 K s^{-1}.

surface.[30] Based on these comparisons and previous work,[9] an analogous bonding and orientation of $C_3H_{5(c)}$ on Cu(100) is proposed (bottom of panel B). In passing, we note that the intensities of the remaining seven A′ modes lie below the detection limit of the MCT detector (peak-to-peak noise ~0.004%).

With the above assessment of the structure taken by the saturated 1:1 η^3-$C_3H_{5(c)}$ and $Cl_{(c)}$ layer, we turn to the central topic of this paper: reaction of C_3H_5Br with this layer. RAIRS spectra after 0.6 L doses of C_3H_5Br, Figure 4, at the indicated temperature reflect the temperature-dependent loss of η^3-$C_3H_{5(c)}$ and gain of 1,5-hexadiene, $C_6H_{10(p)}$. Each spectrum involves a separate surface preparation and was taken at the indicated temperature by scanning RAIRS for 13.5 min immediately after dosing allyl bromide. The reference for these spectra is RAIRS of a $Cl_{(c)}$ layer prepared as described in the Experimental Section.

At 77 K, bands assigned to η^3-$C_3H_{5(c)}$ (886 cm^{-1}) and $C_3H_5Br_{(p)}$ (1213 cm^{-1}) are strong. As the dosing temperature rises, the 1213 cm^{-1} intensity decays to negligible values at 110 K, whereas the 886 cm^{-1} intensity decays between 77 and 110 K but then recovers and broadens. The decays are accompanied the emergence of new bands at 915 and 994 cm^{-1}, assigned unambiguously to 1,5-hexadiene (C_6H_{10}) by comparison with 1,5-hexadiene directly dosed on ~0.2 ML bromine-covered Cu(100) at 110 K.[9] The evidence is clear: at 110 K some, but not all, of the incident flux of C_3H_5Br reacts with η^3-$C_3H_{5(c)}$ to form C_6H_{10} that remains adsorbed.

In striking contrast to the 110 K results, those at 120 K show much less 1,5-hexadiene and more η^3-allyl. Above 130 K, very little 1,5-hexadiene is detected, while the 886 cm^{-1} band of η^3-allyl remains intense but becomes asymmetric with a shoulder at 900 cm^{-1}. We ascribe the shoulder to η^3-allyl perturbed (red-shifted) by $Br_{(c)}$.[23] Above 160 K, RAIRS indicated no changes in the η^3-allyl intensity or line shape as a result of dosing 0.6 L of allyl bromide.

Further insight is gained (Figure 5) by comparing TPD after doses at 110 K of C_3H_5Br (upper panel) and C_6H_{10} (lower panel) on clean and Br-covered (Br prepared as described in the Experimental Section) Cu (100). In each case, the dose exceeds that needed to saturate the first layer. The 121 and 67 amu signals monitor C_3H_5Br and C_6H_{10} desorption, respectively. For a Br-covered surface, C_3H_5Br appears in TPD after dosing C_3H_5Br (spectrum A). The 133 and 146 K peaks are assigned to the second and first layers of C_3H_5Br adsorbed on Br-passivated Cu. Importantly, there is no C_6H_{10} desorption (not shown).

On the other hand, when C_3H_5Br is dosed on clean Cu(100), C_6H_{10} desorbs with peaks at 131 and 148 K (spectrum B). These peaks align with those from directly dosed C_6H_{10}, spectrum C, indicating that a desorption-limited, rather than reaction-limited, process is detected in spectrum B. These TPD results are consistent with RAIRS; C_6H_{10} forms during C_3H_5Br doses at 110 K on clean Cu(100).[9] This highlights an important distinction in the behavior of C_3H_5Cl and C_3H_5Br. Neither RAIRS nor TPD detected 1,5-hexadiene formation from allyl chloride on Cu(100) under any conditions. These reactivity differences are attributable to the C−Cl bond being ~50 kJ mol^{-1} stronger than C−Br.

Comparing TPD of directly dosed C_6H_{10}, spectra C and D, it is clear that ~0.2 ML Br is sufficient to replace the 190 K desorption with a peak at 148 K that has, within 4%, the same peak area. The 190 K peak is attributed to C_6H_{10} in contact with Cu and the 148 K peak to contact with $Br_{(c)}$. In neither case is there evidence for dissociation of C_6H_{10}; i.e., the surface is clean after TPD and no other hydrocarbons or H_2 was detected

(30) Gurevich, A. B.; Teplyakov, A. V.; Yang, M. X.; Bent, B. E.; Holbrook, M. T.; Bare, S. R. *Langmuir* **1998**, *14*, 1419−1427.

in TPD. Finally, the 130 ± 3 K peaks are ascribed to C_6H_{10} adsorbed on itself.

The area of the 148 K peak in spectrum B is 0.65 of that in spectrum C, while the *total* C_6H_{10} desorbing in spectrum B is 0.81 of spectrum C. The results in spectrum B are consistent with the RAIRS data; i.e., reaction to form C_6H_{10} occurs readily at 110 K. The total amount formed is equal, within 20%, to the saturation first layer coverage of C_6H_{10} on clean Cu(100), spectrum D.

IV. Discussion

Coverage of η^3-Allyl, Cl, and Br. On the basis of the CO adsorption results of Figure 1, we estimate the coverage of η^3-allyl as follows. Saturation 1:1 $C_3H_{5(c)}$ and $Cl_{(c)}$ coverage precludes adsorption of CO, whereas the clean surface adsorbs 0.57 CO per surface Cu (0.57 ML), all into atop sites.[25] Removing $C_3H_{5(c)}$ while leaving $Cl_{(c)}$ restores CO uptake capacity to 0.66 of its saturation value (0.38 ML), from which we immediately conclude that $C_3H_{5(c)}$ blocks more CO than $Cl_{(c)}$. Assuming $Cl_{(c)}$ occupies a 4-fold site, as it does when Cl_2 is dosed,[31] and blocks the four surrounding atop sites, we estimate that 0.25 ML of $Cl_{(c)}$ will inhibit all CO uptake. Assuming a linear relation, 0.38 ML of CO implies a Cl coverage of 0.08 ML and, by stoichiometry, an η^3-C_3H_5 coverage of 0.08 ML. Multiplying by 1.53×10^{15} atoms cm^{-2}, the surface atomic density of Cu(100), the estimated absolute coverage of C_3H_5Cl required is 1.2×10^{14} cm^{-2}. This estimate is reasonable compared to the coverage (3.7×10^{14} cm^{-2}) required to pack C_3H_5Cl into a layer equivalent to the density (0.94 g cm^{-3}) of liquid C_3H_5Cl.

Extending this CO titration method, the coverage of Cl (from repeated doses of allyl chloride and annealing cycles) saturates at 0.20 ML, while Br (from allyl bromide) saturates at 0.22 ML. The latter is consistent with the C_6H_{10} TPD data of Figure 5.

Structure and Reactions of η^3-Allyl. The RAIRS results, Figure 2, show that after dosing, annealing to 200 K, and recooling to a selected temperature, allyl chloride has either desorbed or dissociated. We reproduced earlier TPD results[30] showing that for higher temperatures, 470 K, 80% of the initial allyl desorbs; the remaining adsorbed material partially dehydrogenates to hydrogenate neighboring species to form and desorb propylene and an unidentified C_3H_4 species. The $Cl_{(c)}$ desorbs as $CuCl_x$ at ~950 K.

As noted above, vibrational modes are assigned to η^3-C_3H_5 and agree with those from dissociation of allyl bromide on clean Cu(100)[9] and with previous studies of allyl halides on coinage and other transition metal surfaces, as well as organometallic complexes.[26] In addition, there is good agreement between the relative intensities of the observed modes of allyl on Cu(100) and those of a Cr complex (Figure 3).[41]

Comparison of spectra taken at different temperatures indicates that the 947 cm^{-1} band belongs to the $\rho_\omega(CH_2)_{sym}$ mode of η^3-allyl groups strongly perturbed by coadsorbed Cl.[9] This mode in other π-bonded hydrocarbons, such as ethylene and propylene, adsorbed on Cl-modified Ag(111) is sensitive to the presence of halogen atoms, as evidenced by a >30 cm^{-1} blue-shift compared to adsorption on clean Ag(111).[17]

Allyl Bromide Dosed on η^3-$C_3H_{5(c)}$ + $Cl_{(c)}$ at 77 K. When C_3H_5Br is dosed onto η^3-$C_3H_{5(c)}$ + $Cl_{(c)}$ at 77 K, molecular adsorption is clearly evidenced (Figure 4). The band at 1213 cm^{-1} is the $-CH_2$ wag mode of the bromomethyl group.[29] Other allyl halide bands are present: 933 ($=CH_2$ wag), 988 ($=CH_2$ twist), 1194 cm^{-1} ($=CH_2$ rock), and 1638 cm^{-1} (C=C stretch; not shown). These bands are lower by no more than 3−6 cm^{-1} than those observed for solid C_3H_5Br.[29] Further, there is no evidence for dissociation to $C_3H_{5(c)}$ and $Br_{(c)}$, a process readily occurring on clean Cu(100) at 77 K.[9] Not surprisingly, in view of the absence of CO adsorption, we conclude that C_3H_5Br is *physisorbed* onto the η^3-$C_3H_{5(c)}$−$Cl_{(c)}$ adlayer, with negligible interaction with the underlying Cu.

As the dosing temperature is increased, the fall and rise of vibrational intensity associated with η^3-C_3H_5, and the reverse for intensity associated with C_6H_{10}, indicate that the latter's formation is controlled by two temperature-dependent processes. Below 100 K, unreacted allyl bromide accumulates, indicating that the overall C_6H_{10} formation rate is limited by reaction between $C_3H_5Br_{(p)}$ and η^3-$C_3H_{5(c)}$. At 90 K, for example, only 30% of the initial η^3-$C_3H_{5(c)}$ reacts in 100 min (not shown). Between 110 and 160 K, an increasing amount of η^3-$C_3H_{5(c)}$ remains after the C_3H_5Br dose, while the amount of accumulated C_6H_{10} drops. Since the TPD onset for first-layer C_6H_{10} is 130 K and since the RAIRS C_6H_{10} intensity is 30% lower at 120 K than at 110 K, we conclude that the reaction becomes controlled by the $C_3H_5Br_{(p)}$ residence time; i.e., the desorption rate of weakly held allyl bromide becomes competitive with its reaction rate with η^3-$C_3H_{5(c)}$.

Both RAIRS and TPD support the formation of physisorbed 1,5-hexadiene, i.e., $C_6H_{10(p)}$. The peaks in the 110 K RAIR spectrum are within 5 cm^{-1} of those found for C_6H_{10} in the gas phase[32] and adsorbed on halogen-covered Cu(100).[9] Larger shifts occur for C_6H_{10} on clean Cu(100); for example, the CH_2 wagging mode is at 900 cm^{-1}, a shift of 15 cm^{-1} compared to the gas phase (not shown). TPD (Figure 5C,D) shows that the C_6H_{10} desorption energy is higher on clean Cu(100), 190 K peak, than on Br-covered Cu(100), 148 K peak.

As part of the process that forms $C_6H_{10(p)}$, we propose that the Br released occupies sites previously occupied by η^3-$C_3H_{5(c)}$. Such chemical displacement processes are facile on copper surfaces.[33] Based on the peak temperature and a preexponential factor of 10^{13} s^{-1}, the desorption activation energy for C_6H_{10} from clean Cu is 49 kJ mol^{-1}, much weaker than the Cu−Br bond energy, which exceeds 260 kJ mol^{-1} based on TPD, showing that CuBr, not Br, desorbs from Br-covered Cu with a peak at 975 K; i.e., 1,5-hexadiene cannot compete with Br for Cu sites.

Formation of C_6H_{10} has also has been observed on Ag(111) and Ag(110). On Ag(110), formation is interpreted in terms of a Langmuir−Hinshelwood process linking two η^3-$C_3H_{5(c)}$ groups[34] that, in agreement with calculations,[35] is limited by surface diffusion of η^3-$C_3H_{5(c)}$. On Ag(111), C_3H_5Cl and C_3H_5Br dissociate between 77 and 200 K to form η^3-$C_3H_{5(c)}$ that, through two paths, forms C_6H_{10}.[23] Above 200 K, diffusion-limited coupling dominates but, unlike Ag(110), some C_6H_{10} (only from C_3H_5Br) forms and desorbs between 140 and 150 K.[23] The Ag(110) features mimic those reported here, but the yield on Cu(110) is a factor of at least 2 higher for reasons yet to be established.

Precursor Model for Kinetics at T > 110 K. In view of the competition between reaction and desorption of C_3H_5Br, we apply a simple precursor model to the RAIRS data, Figure

(31) Nakakura, C. Y.; Zheng, G.; Altman, E. I. *Surf. Sci.* **1998**, *401*, 173−184.

(32) NIST Chemistry Web Book; http://webbbok.nist.gov/chemistry/.

(33) Kash, P. W.; Yang, M. X.; Teplyakov, A. V.; Flynn, G. W.; Bent, B. E. *J. Phys. Chem. B* **1997**, *101*, 7908−7918.

(34) Carter, N. R.; Anton, A. B.; Apai, G.*J. Am. Chem. Soc.*, **1992**, *114*, 4410−4411.

(35) Shustorovich, E. *Surf. Sci.* **1992**, *279*, 355−366.

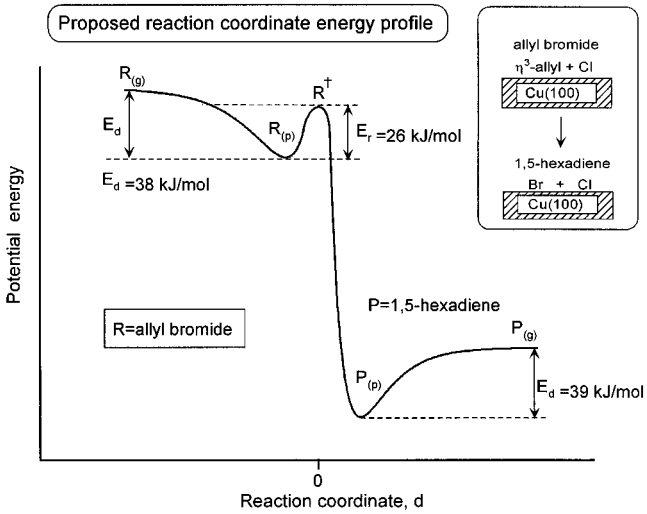

Figure 6. Schematic one-dimensional potential energy profile for the reaction, illustrated in the inset, of $C_3H_5Br_{(g)}$, denoted $R_{(g)}$, with η^3-$C_3H_{5(c)}$ to form $C_6H_{10(g)}$, denoted $P_{(g)}$. Adsorption first forms $R_{(p)}$ that is physisorbed over the 1:1 mixture of η^3-$C_3H_{5(c)}$ and Cl(c). In competition with desorption, thermal activation of $R_{(p)}$ forms a transition state, denoted $R^{\dagger}$, from which product $P_{(p)}$, physisorbed 1,5-hexadiene adsorbed on $Cl_{(c)} + Br_{(c)}$, is synthesized.

6. Along the reaction coordinate, the adsorbed reactant complex, $R_{(p)}$, defined as $C_3H_5Br_{(p)}$ physisorbed on η^3-$C_3H_{5(c)}$ mixed with $Cl_{(c)}$, passes through a transition state barrier at $d = 0$ to form the adsorbed product complex, $P_{(p)}$, defined as $C_6H_{10(p)}$ physisorbed on $Cl_{(c)}$ mixed with $Br_{(c)}$. The inset schematically illustrates the structural transformation.

Integrated intensities, I, of the 886 cm^{-1} wagging mode of η^3-$C_3H_{5(c)}$ are used to describe the extent of reaction involved in the fixed doses of C_3H_5Br at the selected substrate temperatures (Figure 4). An average reaction probability (S_r) characterizing the C_3H_5Br dose is defined as

$$S_r = \frac{(I^\circ - I)}{I^\circ} \tag{2}$$

where I° and I are intensities measured before and after dosing C_3H_5Br (Figure 4). In calibration experiments based on TPD of C_3H_5, we demonstrated that the RAIRS intensity increases linearly with the η^3-$C_3H_{5(c)}$ coverage. The expected uncertainty in S_r is determined by the signal-to-noise ratio (SNR) of the RAIR band. The average SNR of the CH_2 wagging mode of η^3-C_3H_5 is ~35 (Figure 2).

For data taken between 85 and 160 K, S_r rises from 0.04 to 0.62 between 85 and 110 K and then falls to 0.03 at 160 K (Figure 7). At 85 K the reaction rate is neglible; only 4% of the η^3-allyl reacted in 16 min. At 110 K, no allyl bromide accumulates and, based on $S_r = 0.62$, 62% of the initial η^3-allyl coverage (0.08 ML) reacted to form 1,5-hexadiene.

The decay of S_r above 110 K is taken as a signature of a precursor-mediated surface process analyzable using the following phenomenological rate equations:

$$C_3H_5Br_{(g)} - \alpha F \rightarrow C_3H_5Br_{(p)}$$

$$C_3H_5Br_{(p)} - k_d \rightarrow C_3H_5Br_{(g)}$$

$$C_3H_5Br_{(p)} + \eta^3\text{-}C_3H_{5(c)} - k_r \rightarrow C_6H_{10(p)} + Br_{(c)}$$

where α is the trapping probability of C_3H_5Br into a physisorbed state and F is the incident flux of C_3H_5Br. The rate coefficients, k_d and k_r, describe C_3H_5Br desorption and reaction, respectively.

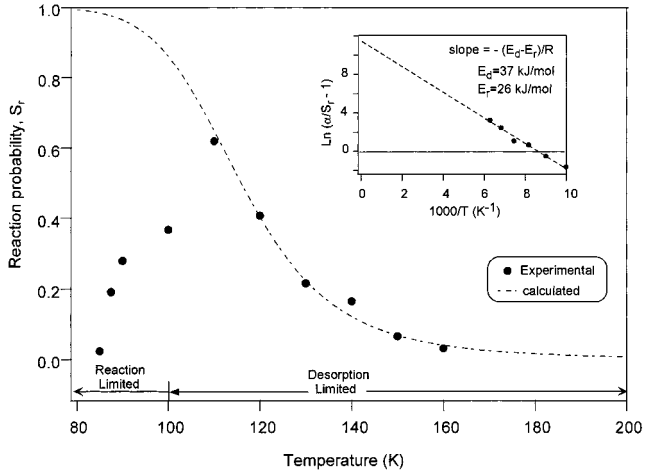

Figure 7. On a Cu(100) surface, the reaction probability, S_r, as a function of temperature, for the C−C bond-forming reaction that synthesizes 1,5-hexadiene from physisorbed C_3H_5Br reacting with chemisorbed η^3-$C_3H_{5(c)}$. The dashed line is the calculated reaction probability. The inset is an Arrhenius plot based on eq 4 for reaction temperatures between 110 and 160 K, and a linear fit (dashed line) is also shown.

Since RAIRS shows no C_3H_5Br accumulation above 110 K, it either reacts with η^3-$C_3H_{5(c)}$ or desorbs into the gas phase during the 150 s dose. Under these conditions, the instantaneous coverage of physisorbed C_3H_5Br, θ_p, is very small and a steady-state approximation is valid, i.e., $(d\theta_p/dt) = 0.0$. Under these conditions, the reaction probability, S_r, is given by the ratio between the rate of reaction (R_r) and the impinging flux (F). Straightforward algebraic manipulation gives

$$S_r = \alpha\left(\frac{k_r}{k_r + k_d}\right) = \frac{\alpha}{1 + k_d/k_r} \tag{3}$$

The reaction probability is given by the product of the trapping probability α and, once trapped, the fraction of C_3H_5Br that reacts. Because the stoichiometry is 1:1, P_r is also the reaction probability of η^3-$C_3H_{5(c)}$. Taking the Polanyi−Wigner form for both k_r and k_d, the temperature dependence of P_r is given by

$$S_r = \frac{\alpha}{1 + \left(\frac{k_d^{(0)}}{k_r^{(0)}}\right) e^{-(E_d - E_r)/RT}} \tag{4}$$

Following previous work,[6] we assume the trapping probability is unity and temperature independent. This is not unreasonable since the average incident translational energy of $C_3H_5Br_{(g)}$ is less than one-third of the physisorption well depth for $C_3H_5Br_{(p)}$.

Using eq 4, a plot of $\ln[(\alpha/S_r) - 1]$ as a function of T^{-1} is nicely linear (inset of Figure 7), and from the slope, $E_d - E_r = 12$ kJ mol^{-1}; from the intercept, $k_d^{(0)}/k_r^{(0)} = 9.4 \times 10^4$. These values were used to construct the dashed curve through the data (and the extrapolation) in the body of Figure 5. Using Redhead analysis[36] with $k_d^{(0)} = 10^{13}$ s^{-1}, and data for TPD of $C_3H_5Br_{(p)}$ on ~0.2 ML Br-covered Cu(100) (Figure 5), the calculated desorption activation energy is 38 kJ mol^{-1}. This is a suitable estimate for E_d in the case where desorption occurs from η^3-$C_3H_{5(c)}$ mixed with $Cl_{(c)}$, i.e., $k_d = 10^{13} \exp\{-38 \text{ kJ mol}^{-1}/RT\}$ s^{-1}. From this, $k_r = 1.1 \times 10^8 \exp\{-26 \text{ kJ mol}^{-1}/RT\}$ s^{-1}. Table 1 summarizes the rate parameters for desorption and reaction

(36) Redhead, P. A. *Vacuum* **1962**, *12*, 203−211.

Table 1. Experimentally Determined Rate Parameters

adsorbate	E_d (kJ mol^{-1})	$k_d^{(0)}$ (s^{-1})[a]	E_r (kJ mol^{-1})	$k_r^{(0)}$ (s^{-1})
allyl bromide	38	10^{13}	26	1×10^8
1,5-hexadiene	39	10^{13}	241.4[c]	6×10^{14} [c]
η^3-allyl	107	10^{13}	na[d]	na
$Cl_{(c)}$[b]	250	10^{13}	na	na
Br(c)[b]	260	10^{13}	na	na

[a] Assumed values. [b] Reference 39. [c] Central C−C bond scission in gas phase; ref 37. [d] na, not applicable.

including parameters for the formation of allyl radicals from the thermal decomposition of 1,5-hexadiene[37] and the desorption energies of chemisorbed Br and Cl atoms from Cu(100).[38]

As anticipated for precursor-assisted reactions,[39] the experimental reaction probability (Figure 7) decreases as the surface temperature increases since, with respect to the bottom of the physisorption potential energy well, the barrier to desorption ($E_d = 38$ kJ mol^{-1}) is about the same as the barrier to reaction with η^3-$C_3H_{5(c)}$ ($E_r = 26$ kJ mol^{-1}). In a one-dimensional representation (Figure 6), the activated complex, $R^\dagger = C_3H_5Br \cdots \eta^3$-$C_3H_{5(c)}$, lies 26 kJ mol^{-1} above $R_{(p)}$.

The reaction probabilities in Figure 7 indicate that the reaction does not occur via a direct mechanism; i.e., C_3H_5Br does not react on the inbound trajectory. Rather, energy is transferred to a trapped adsorbate state, and a reaction, competing with desorption, occurs from this state. The fit to the extrinsic precursor model is certainly adequate.

Proposed Electron-Transfer Mechanism. The reaction described here has analogues in organometallic chemistry: transition metal-catalyzed carbon−carbon bond-forming reactions between organometallic nucleophiles and organic halide electrophiles are common (Scheme 1).[40] These proceed by electron transfer from the nucleophile to the carbon−halogen bond and subsequent formation of a radical anion intermediate. For example, organic halides (RX) react with (η^3-allyl)-nickel halides in a so-called nucleophilic radical chain reaction, $S_{RN}1$, mechanism that involves the short-lived ($\sim$1 μs) radical anion, RX^-.[41] While the time scale of the RAIRS measurements does not allow determination of whether electron transfer, bond breaking, and bond formation are concerted or stepwise, we propose that the surface reaction reported here involves an electron transfer from η^3-$C_3H_{5(c)}$ to the C−Br bond of $C_3H_5Br_{(p)}$ that results in the transient formation of $C_3H_5Br^-$. The latter reacts, with significant probability, with the surface η^3-$C_3H_{5(c)}$ to form 1,5-hexadiene, $C_6H_{10(p)}$, and $Br_{(c)}$. The physisorbed state of 1,5-hexadiene is the result of chemical displacement by the more aggressive bromine atom, as discussed above.

Scheme 1

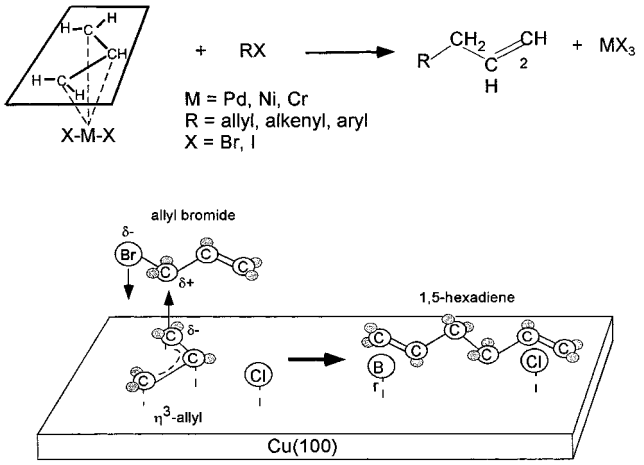

IV. Conclusion

The reaction between chemisorbed η^3-allyl, $C_3H_{5(c)}$, and transiently physisorbed allyl bromide, $C_3H_5Br_{(p)}$, to form adsorbed 1,5-hexadiene, $C_6H_{10(p)}$, has been characterized by RAIRS and TPD. Between 110 and 160 K, the kinetics are described in terms of an extrinsic precursor trapping-mediated model. As expected for such a model, the reaction probability decreases rapidly with increasing substrate temperature. The difference in the activation energies for desorption and reaction of $C_3H_5Br_{(p)}$ ($E_d - E_r$) is 12 kJ mol^{-1}. We expect this to be generalizable to other metal surfaces under conditions where η^3-$C_3H_{5(c)}$ forms and the activation energy for reaction with electrophiles, e.g., organic halides, is low enough to compete with alternative reaction paths, e.g., desorption and decomposition of η^3-$C_3H_{5(c)}$.

Acknowledgment. This work was supported in part by the Robert A. Welch Foundation and by the U.S. Department of Energy, Office of Basic Energy Sciences. We also thank Professor Buddie Mullins and C. Reeves for helpful discussions.

JA0011414

(37) Roth, W. R.; Bauer, F.; Beitat, A.; Ebbrecht, T.; Wüstefeld, M. *Chem. Ber.* **1991**, *124*, 1453−1460.
(38) Nakakura, C. Y.; Phanse, V. M.; Altman, E. I. *Surf. Sci.* **1997**, *370*, L149−L157.
(39) Rettner, C. T.; Ashfold, M. N. R. *Dynamics of Gas−Surface Interactions*; Royal Society of Chemistry: London, 1991.
(40) Hegedus, L. S.; Thompson, D. H. P. *J. Am. Chem. Soc.* **1985**, *107*, 5663−5669.
(41) Swang, O.; Blom, R. *J. Organomet Chem.* **1998**, *561*, 29−35.
(42) Goddard, R.; Krüger, C.; Mark, F.; Stansfield; R.; Zhang X. *Organometallics* **1985**, *4*, 285−290.